ANALYSIS OF THE POLYMERASE CHAIN REACTION PERFORMANCE IN THE NATURAL CONVECTION

ŽIGA VAUPOTIČ

Faculty Jožeta Plečnika

Research paper
Biofluid mechanics

Ljubljana 2023

Abstract
This research paper focuses on analyzing the potential use of natural convection as an alternative or primary method for temperature control in polymerase chain reaction (PCR). PCR is used to amplify copies of DNA and is considered to be one of the most important processes of molecular biology. Computational fluid dynamics(CFD) simulations will be used to model and analyze the thermal behavior of PCR systems. The usage of such methods is a great alternative to experimental data. The research seeks to understand the temperature distribution in the natural convection PCR system. Hence, provide a great insight into the yet unclear connection between natural convection and PCR efficiency. The results will have many applications, such as enhancing the efficiency, efficacy and performance of PCR machines

Keywords: *Polymerase chain reaction, TAQ polymerase chain reaction, natural convection, computational fluid dynamics, DNA copying*

Contents

1. Introduction **5**
1.1 Purpose of the study 5

2. Biomolecular structure **6**
2.1 Initial mixture 6
2.2 PCR phases 7

3. Mathematical structure **8**
3.1 Physical properties 8
3.1.1 Laminar Flow 8
3.1.2 Turbulent Flow 8
3.2 Convection equations 8
3.3 Numerical method 10
3.4 Hyper Viscous Term 11

4. Results and discussion **11**
4.1 Convection in a capillary tube 12
4.1.1 Turbulent System 13
4.2 Convection in an enclosed loop 14
4.2.1 Triangular loop 14
4.2.2 Rectangular and circular loop 15
4.3 Convection in a disk 16
4.4 Performance analysis of the convection systems 16

5. Conclusions **17**
5.1 Further development 17

List of Figures

1 Denaturation phase of the PCR 7
2 Annealing phase of the PCR 7
3 Extension phase of the PCR 7
4 CCPCR at 60s 12
5 CCPCR at 90s 12
6 CCPCR at t>120s 12
7 TCCPCR at 60s 13
8 TCCPCR at 90s 13
9 TCCPCR at t>120s 13
10 Triangluar CPCR 14
11 Unstable Rectangular RLCPCR 15
12 Unstable Circular RLCPCR 15
13 Stable Circular RLCPCR 15

Acronyms

CFD Computational fluid dynamics. 2, 5, 17

CPCR Convective polymerase chain reaction. 13, 17

DNA Deoxyribonucleic acid. 2, 5–8, 12

dNTP Deoxynucleoside triphosphate. 6, 7

FVD Finite Volume Method. 5

PCR Polymerase chain reaction. 2, 5–8, 11–14, 17

TAQ Thermostable *(PCR)* named after Thermus aquaticus. 6, 8

1. Introduction

The polymerase chain reaction (PCR) has revolutionized molecular biology and various scientific disciplines by providing a powerful tool for copying specific DNA sequences. Accurate temperature control is necessary during the PCR process. Thermocyclers are employed to precisely regulate temperature cycles, but they can be expensive and require significant power consumption. In recent years, natural convection has emerged as a promising alternative for temperature control in PCR, as it offers potential energy efficiency and cost savings. This research paper aims to analyze the performance of PCR under natural convection conditions using computational fluid dynamics(CFD). By studying the thermal effects of natural convection on PCR performance, we seek to evaluate the feasibility and effectiveness of natural convection as a viable alternative for maintaining stable and uniform temperatures during PCR.

CFD simulations provide a powerful tool for investigating fluid flow and heat transfer phenomena, making them suitable for analyzing the thermal behavior of PCR systems. By leveraging the capabilities of CFD, we can model and study the complex fluid dynamics and heat transfer mechanisms that occur during PCR. These simulations allow us to visualize and analyze temperature distribution, flow patterns, and heat transfer rates within the reaction system, providing valuable insights into the effects of natural convection on PCR performance.

One crucial aspect of PCR performance is the accurate and uniform distribution of temperature within the reaction mixture. Temperature variations can lead to incomplete or inaccurate amplification, compromising the reliability and accuracy of PCR results. Natural convection dictates temperature distribution within the reaction system. Understanding the impact of natural convection on temperature profiles is crucial for optimizing PCR performance.

To conduct this research, we will develop a computational model that simulates the fluid flow and heat transfer in a PCR system under natural convection conditions. The model will be based on a Finite Volume Method *(FVD)*. We will derive a set of equations describing the physical properties of the PCR in natural convection.

The findings of this research will provide valuable insights into the connection between natural convection and PCR performance. By relying solely on CFD simulations, we can thoroughly investigate the thermal effects of natural convection without the constraints of experimental limitations.

1.1 Purpose of the study

The outcomes of this research will have significant implications for the design and optimization of PCR systems. The findings can guide the development of PCR devices that use natural convection for efficient temperature control, leading to cost-effective, energy-efficient solutions. Furthermore, these advancements can facilitate the integration of PCR technology into portable diagnostic platforms and resource-limited settings, enhancing the accessibility and affordability of molecular diagnostics. Which are of great importance for countries in development.

2. Biomolecular structure

Polymerase Chain Reaction is a technique in molecular biology that allows for the amplification of specific segments of DNA. It has transformed the field of genetic research in early 1990. By repeatedly cycling through a series of heating and cooling steps, PCR can generate millions of copies of a target DNA sequence.

PCR was originally developed for the detection of mutations in the HBB gene causing sickle cell anemia and by mistake revolutionized the field of molecular biology. This breakthrough involved the enzymatic amplification of the -globin gene using radioactive-labeled oligonucleotides and restriction analysis to identify inherited mutations. Later on, PCR was then utilized for genotyping HLA-DQ alleles. Subsequently, PCR found widespread clinical use in fields such as clinical genetics and microbiology, enabling the detection of viral and bacterial infections. The finding of multiplex PCR, allows simultaneous amplification of amplicons of different lengths and laid the foundation for large gene panel libraries used in next-generation sequencing. Another significant advancement occurred when TAQ PCR was employed to amplify DNA from single sperm cells [1], leading to its application in forensic science and assisted reproduction [2]. PCR became fully quantitative with the development of real-time monitoring techniques, enabling the precise analysis of nucleic acids. This led to the emergence of qPCR and RT-PCR (reverse transcription PCR) for RNA studies, which became the gold standard for quantitative nucleic acid analysis. In addition to end-point PCR, qPCR, and digital PCR (dPCR), various PCR variants have also been developed, including bridge PCR [3]. The scope of this research paper's interest is mainly the usage of TAQ PCR for the amplification of DNA.

2.1 Initial mixture

The basic procedure of polymerase chain reaction is fairly simple and involves a series of steps. Initially, the DNA sample is collected and prepared for amplification. To initiate the amplification process, the DNA sample must first be mixed with a deoxynucleoside triphosphate (dNTP) set, which includes dATP, dGTP, dCTP, and dTTP. These dNTPs, also known as free nucleotides, serve as the building blocks for DNA replication [4].

Next, a pair of oligonucleotide primers is added to the mixture. These primers are short DNA sequences that are designed to be complementary to the 5' and 3' ends of the target DNA template. They provide a starting point for DNA polymerase to initiate replication and amplify the desired DNA region.

The DNA polymerase, usually TAQ polymerase, is then included in the reaction mixture. TAQ polymerase is derived from the bacterium Thermus aquaticus and is capable of withstanding the high temperatures required for the PCR process. It is responsible for synthesizing new DNA strands by adding complementary nucleotides to the primers.

To ensure optimal conditions for the PCR reaction, a reaction buffer is added to the mixture. The buffer maintains the pH and ion concentration at appropriate levels throughout the reaction, providing a stable environment for the DNA polymerase to function effectively.

Additionally, cofactors such as magnesium ions (Mg^{2+}) are included in the reaction mixture. Magnesium ions are essential for activating the TAQ polymerase and enabling its enzymatic activity during DNA replication.

2.2 PCR phases

After the assembly of the initial mixture, the three copying phases take place:

1. **Denaturation phase** - In the denaturation phase, the PCR reaction mixture is heated to a high temperature, typically around 94°C. The purpose of this step is to separate the double-stranded DNA into two single strands. At elevated temperatures, the hydrogen bonds between the complementary base pairs (A-T and G-C) holding the DNA strands together are broken, resulting in the denaturation of the DNA template. [5]

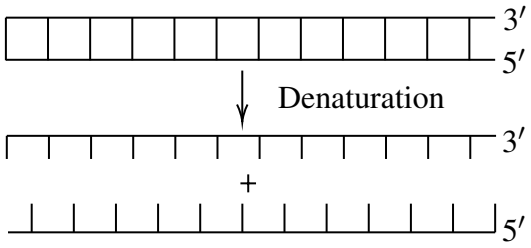

Figure 1. Denaturation phase of the PCR

2. **Annealing phase** - After denaturation, the reaction mixture is cooled to a temperature ranging from 50°C to 65°C. This temperature allows the primers to anneal or bind to their complementary sequences on the single-stranded DNA template. The primers are designed to be specific to the target DNA region, enabling them to hybridize to the desired template sequence. [5]

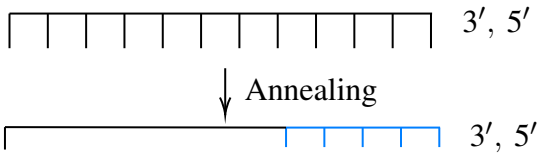

Figure 2. Annealing phase of the PCR

3. **Extending** - Once the primers have successfully annealed to the DNA template, the temperature is raised to around 70°C to 75°C. At this temperature, the DNA polymerase, along with the added dNTP s (deoxynucleotide triphosphates), extends the primers by synthesizing new DNA strands complementary to the template. The DNA polymerase enzyme catalyzes the addition of the appropriate dNTP s (dATP, dGTP, dCTP, and dTTP) to the growing DNA strands, following the complementary base-pairing rules.

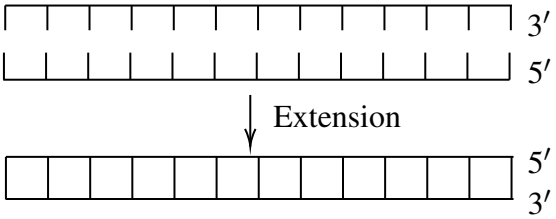

Figure 3. Extension phase of the PCR

The PCR cycle amount depends on the template of DNA, the reaction mix, and the expected yield of the product. Usually, the mixture is put through $25-40$ cycles. After the last cycle, the samples must be incubated at 72 $^{\circ}C$ for $5-15$ minutes. The incubation phase allows TAQ Polymerase to add an extra nucleotide to the 3'-ends of the products.[6]

3. Mathematical structure

The first mention of natural convection-driven PCR namely CPPCR was introduced by Hwang et al [7] in early 2000s. The yet unknown potential of such PCR procedure was quickly unrevealed through the next years. Usually, a very simple form of convection called Rayleigh Benard convection is used [8]. The Rayleigh Benard (RB) convection occurs when the fluid is heated from below and cooled from above. The temperature difference between the top and bottom surfaces leads to density variations, which drive the formation of convection cells or rolls in the fluid [9]. This sometimes leads to the formation of stable RB convection cells (Benard cells) where liquid flows in circles through the system and meanwhile creates a cell-like shape [10].

Convection is usually divided into two main modes. The two modes are represented by the flow's turbulent characteristic. Usually, PCR is only performed in the so-called laminar mode, where multiple PCR layers move up and down through the system essentially going through all the PCR phases due to the heat change. Recent studies have shown that instead a much more complex and turbulent (chaotic advection) mode can be used to accelerate the DNA amplification. [11]

3.1 Physical properties

3.1.1 Laminar Flow

As already mentioned, usually the laminar flow is used. The only problem with laminar flow is that it is hard to ensure, as the temperatures are very large. For example, flows that exceed $Ra > 10^6$ [12] are usually considered turbulent (Check 11th equation for the definition of Ra). The designs of laminar flow natural convection are greatly described in [13].

3.1.2 Turbulent Flow

Turbulent flows include fluid flow where irregular and chaotic motion is present. Due to its nature, the thermal stability of such flows is usually not present. Hence, many recent research papers have shown that this could greatly impact the quality and the speed of the PCR. For example in the research [14] one of the first turbulent systems was proven to be successful. Earlier papers such as [15] have proposed much simpler yet still effective designs.

3.2 Convection equations

The convection will be placed in a container full of liquid. The liquid can therefore be assumed incompressible. Moreover, we describe the flow of the liquid in the container using the Cauchy momentum equation [16].

$$\rho \frac{Du}{Dt} = -\nabla p + \nabla \cdot \tau + f_{out} \tag{1}$$

(u is liquid velocity vector field, τ is the stress tensor, p is pressure scalar field, f_{out} are outside forces, ρ is the initial density of the liquid)

Note: The derivative $\frac{D}{Dt}$ is usually called material derivative and is used in such form

$$\frac{D}{Dt} = \frac{\partial}{\partial t} + u \cdot \nabla. \tag{2}$$

Since the liquid in consideration is mainly water, we can assume that the liquid is Newtonian. Therefore the stress tensor τ is a normal viscous tensor and can be written in the form

$$\tau = \mu \nabla^2 u, \tag{3}$$

(μ is dynamic viscosity). We have derived the incompressible Navier-Stokes equation

$$\rho \frac{Du}{Dt} = -\nabla p + \mu \nabla^2 u + f_{out}. \tag{4}$$

The continuity equation must not be disregarded. The standard continuity equation can be written in the form

$$\frac{D\rho}{Dt} + \rho(\nabla \cdot u) = 0. \tag{5}$$

Since we had already assumed the liquid to be incompressible, the equation generalizes into

$$\nabla \cdot u = 0. \tag{6}$$

The conservation and distribution of the heat throughout the liquid can easily be described using the convection-diffusion equations

$$\rho Cp \frac{DT}{Dt} = \nabla \cdot (\lambda \nabla T) + \Phi, \tag{7}$$

(Cp is specific heat capacity, λ is thermal conductivity constant). We can disregard Φ or the heating from the microscopic effect of viscous dissipation, as we expect it to be $\Phi \approx 0$ [17]. The rest of the equation can therefore be written in the following form

$$\frac{\partial T}{\partial t} + u \cdot \nabla T = \frac{\lambda}{\rho Cp} \nabla^2 T. \tag{8}$$

The last thing that we must consider is the connection between the convection-diffusion equations and the Navier-Stokes equation. We can do that by using the Boussinesq approximation. The density difference is said to be so small $\left\| \frac{\Delta\rho}{\rho} \right\| \ll 1$ that it can be disregarded on every part of the Navier-Stokes equation besides the outer-forces part which is ultimately responsible for the flow of the liquid. The approximation arises from the fact that the inner acceleration of the liquid is much smaller than the acceleration of the liquid by the outside forces. The outside forces f_{out} are therefore written in the form

$$f_{out} = \Delta\rho g = -\rho\beta(T - T_{ref})g\hat{j}, \tag{9}$$

(β is the volumetric thermal expansions coefficient and T_{ref} is a reference temperature, $\hat{j}$ is a unit vector pointing in y direction).

Let $\Omega \subset \mathbb{R}^2$ be a bounded domain of the system. Thus, the following system is considered for every $t > 0$

$$\begin{cases} \dfrac{Du}{Dt} = -\dfrac{1}{\rho}\nabla p + \mu\nabla^2 u + g\hat{j}\beta(T - T_{ref}) \\ \nabla \cdot u = 0 \\ \dfrac{DT}{Dt} = \dfrac{\lambda}{\rho C p}\nabla^2 T. \end{cases} \tag{10}$$

In the following sections, two dimensionless numbers will be used. Firstly, Rayleigh Number which is given by

$$Ra = \frac{g\beta\rho^2 l^3 (T_1 - T_0)}{\lambda\mu}. \tag{11}$$

Secondly, Reynolds number which is given by the equation

$$Re = \frac{\rho\overline{||u||}_2 l}{\mu} \quad Re_m = \frac{\rho(\max_{(x,y)\in\Omega}||u||_2)l}{\mu}. \tag{12}$$

Last, but not least the Nusselt number will be used. The number measures the ratio between convective and conductive heat transfer [18].

$$Nu = 1 + \int_{\partial\Omega} Tu \cdot \vec{dS} \tag{13}$$

3.3 Numerical method

For the best results, we must use a fully conservative numerical approximation. We will use a locally conservative method called *Finite Volume Method* [19]. We must discretize the domain Ω in n so-called control volumes denoted by $V_i \subset \Omega$, where $0 < i \leqslant n$, such that

$$\bigcup_{i=1}^{n} V_i = \Omega \qquad \bigcap_{i=1}^{n} V_i = \varnothing. \tag{14}$$

The general solution will represent the solutions of all control volumes. For each control volume, we must ensure the continuity equation and full conservation of energy. Thus, we should write the equations in the integral form, so the fluxes on all the bounds of the control volume cancel out. The flux integrals can be obtained using the divergence theorem. We can approximate the solutions of the surface integrals using the midpoint rule.

$$\int_{\partial V_i} u \cdot \vec{dS} = \sum_{\mathbf{S_i}\subset\partial\mathbf{V_i}} n_i \cdot u\Delta S_i. \tag{15}$$

The rest of the derivatives can be written in the form of a finite difference scheme. Hence, the integral form of terms, that can't be turned into a surface integral can be approximated as such

$$\int_{V_i} \frac{\partial u}{\partial t} dV = \frac{u^{N+1} - u^N}{\Delta t}\Delta V. \tag{16}$$

The pressure gradiant can be calculated using the pressure projection method. Using the Helmholtz decomposition we can fastly derive the pressure Poisson equation (*Note: $\widetilde{u}$ is the calculated velocity field without the pressure gradient*).

$$\nabla^2 p = \frac{\nabla \cdot \widetilde{u}_{i,j}}{\Delta t}. \tag{17}$$

The convergence issues caused by the pressure projection method can easily be resolved using the staggered grid. The staggered grid is obtained by shifting pressure gradient discrete points in comparison to the liquid velocity field discrete points.

3.4 Hyper Viscous Term

We quickly notice that natural convection with large numbers produces an unstable and turbulent system. Even the system with smaller numbers($Ra \approx 10^6$) produces turbulent results.

Usually, such schemes become so unstable at $Ra > 10^7$ that the solution is unobtainable. Many stabilizing factors have been proposed through the years. For the purpose of the study and the complex geometry used, the so-called "Hyper-viscosity" term will be used [20]. A higher-order artificial Laplacian term is added to the Navier-Stokes equation as a regularization factor. General formual for a laplacian of a function $f \in C^{2\alpha}(\mathbb{R}^2)$ is

$$\nabla^{2\alpha} f = \sum_{i=0}^{\alpha} \binom{\alpha}{i} \frac{\partial^{2\alpha}}{\partial x_1^{2i} \partial x_2^{2(\alpha-i)}}[f]. \tag{18}$$

Let ∇^4 denote a second-order Laplacian operator, given by the

$$\nabla^4 f = \frac{\partial^4 f}{\partial x^4} + \frac{\partial^4 f}{\partial y^4} + \frac{\partial^4 f}{\partial x^2 y^2} + + \frac{\partial^4 f}{\partial y^2 x^2}. \tag{19}$$

Let ε be a small hyper viscous constant. The Navier-Stokes equation is now given by

$$\frac{Du}{Dt} = -\frac{1}{\rho_0}\nabla p + \mu \nabla^2 u + g\hat{j}\beta(T - T_{ref}) + \varepsilon \nabla^4 u. \tag{20}$$

4. Results and discussion

In this section, we will analyze the designs of natural convection-driven PCRs. Most of the simulations were performed in Python based on the derived algorithm. For complex geometries, C++ Medusa library was used [21]. The derived finite volume method uses predefined mesh while Medusa uses meshless algorithms to fill the grid with discrete points. RBF-FD [22] has been used as a primary algorithm for numerical approximation with Medusa library.

The results will be compared to non-convective PCR systems. The designs and structure of the following convection-driven PCRs are described in [11]. Usually, the PCR mixture consists mainly of water and therefore the simulation parameters will be those of water. The results will be compared mainly based on the heat distribution, Rayleigh number, Nusselt number and the speed of the fluid.

C_p	$4200J$
λ	$0.6\frac{W}{mK}$
ρ	$1000\frac{kg}{m^3}$
g	$9.8\frac{m}{s^2}$
μ	$9.1 \cdot 10^{-}3\frac{kg}{ms}$
β	$207 \cdot 10^{-}6\frac{1}{K}$

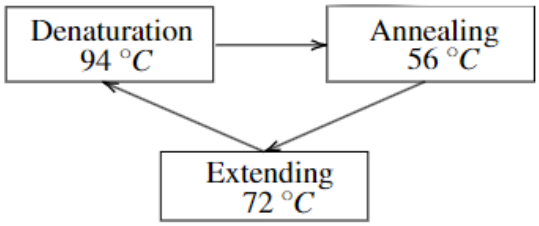

4.1 Convection in a capillary tube

A capillary convective PCR platform (CCPCR) is the most common system for PCR in natural convection. In the aforementioned technique, a capillary tube is used. The tube is usually placed horizontally [23], but vertical designs have also been made [24]. For the purpose of this study, the tube will be horizontally aligned. The bottom of the tube is usually heated to 94°, while the top part is either heated to $56^{\circ}C$ or stays at room temperature. The heat establishes a simple Rayleigh Benard convection [11]. The convection creates a system where the PCR mixture flows in circles throughout the whole tube. A stable heat distribution is usually considered, although it has been shown that turbulent convection can also greatly affect the speed and the quality of the PCR [25]. Let $\Omega = [0, 0.023] \times [0, 0.02]$ be a bounded domain of the following system:

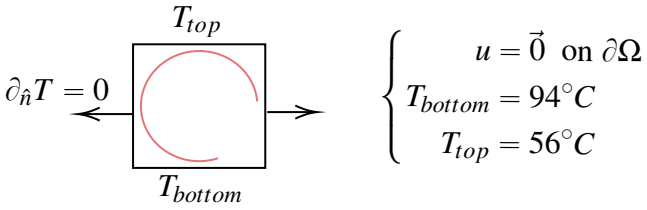

Standard Neumann boundary conditions are applied to the left and right walls $\frac{\partial T}{\partial \hat{n}} = 0$.

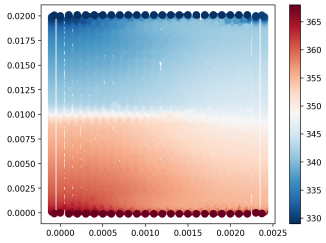

Figure 4. CCPCR at 60s

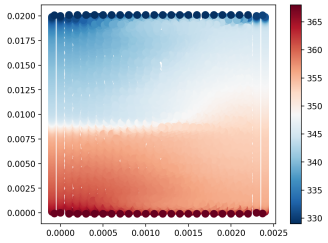

Figure 5. CCPCR at 90s

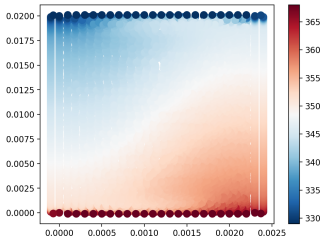

Figure 6. CCPCR at t>120s

The Figure 4.,5. and 6. clearly show that the system is stable. The heat distribution is not changing much instead it allows for a nice laminar convective fluid flow. Usually, each PCR cycle (all three phases) takes 3-5 minutes, here cycle time differed based on the DNA position in the convection, therefore the time must be well controlled as when the cycle number exceeds 45 circles nonspecific bonds are being created. [26].

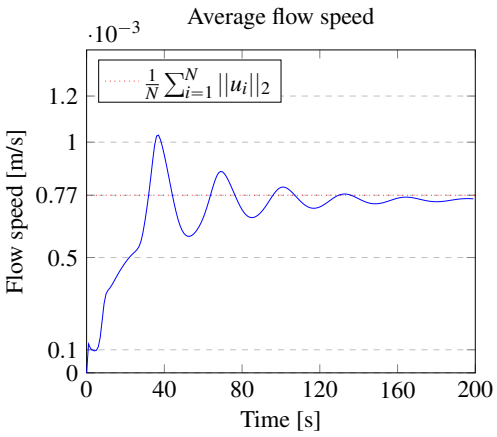

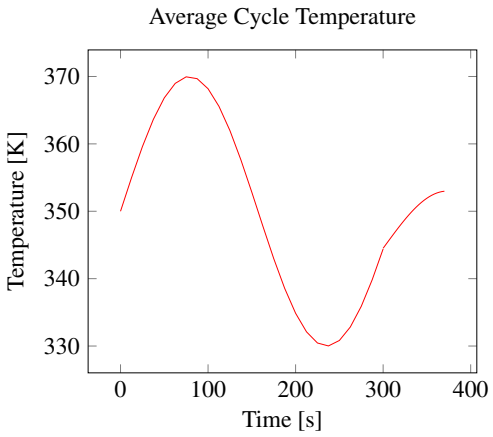

The maximum value of a cycle time at a somewhat constant speed $(t > 200s)$ is around $480s$, average time is on point with a non-convective PCR at $370s$. What is often disregarded is that while the circle time is similar, the convection is slightly faster as the cycle time on none convective PCRs excludes the cooling phases. As for the heat analysis, we can clearly see that every part of the fluid undergoes a heat phase change. The PCR must be preheated for at least 2 minutes as seen by the picture, as by then the convection becomes very stable and does not have an osculating behavior like at the start (*Note: occasional unsmooth graph behavior is usually a byproduct of hyper viscosity*).

Sometimes a slightly different scheme is considered [23]. Instead of heating the fluid from the bottom and the top, we heat the fluid at annealing temperatures at the top and the bottom, as well as heat the fluid at denaturation temperatures on the left and right boundaries. Similar results are expected.

4.1.1 Turbulent System

The instability at high Ra numbers in CCPCR systems can be exploited for a turbulent CPCR design. The quick temperature changes can quickly accelerate the cycle number. Moreover, the turbulent system produces quick results. Unfortunately, the expected yield has not yet been researched, and therefore we can not be sure if such PCRs are also as effective as none turbulent CPCRs and traditional PCRs. The following design will use similar parameters as those of the laminar CCPCR system. The first usage of a turbulent PCR system was proposed by the study [15]. Consider the following domain $\Omega = [0,002] \times [0,0.02]$.

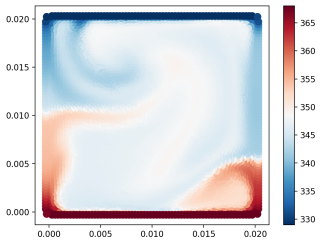

Figure 7. TCCPCR at 60s

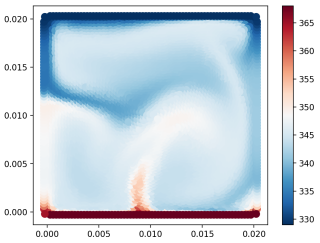

Figure 8. TCCPCR at 90s

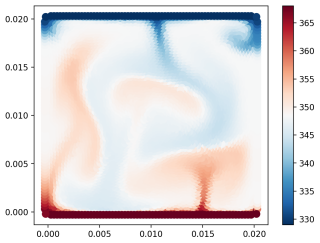

Figure 9. TCCPCR at t>120s

One can clearly see by Figure 7,8,9 that the flow is turbulent and unordered. This means that the speed is also unstable, providing a fully unstable system as seen by the graph. Heat distribution and thus cycle amount is quickly changing meaning one must be very careful. The average cycle temperature was calculated on the region $\Gamma = \{(x,y) \in \mathbb{R}^2 : x^2 + y^2 = 0.01^2\}$

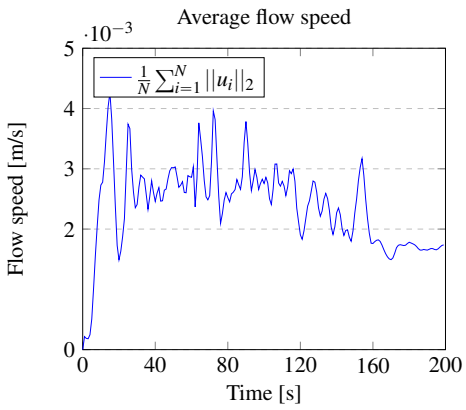

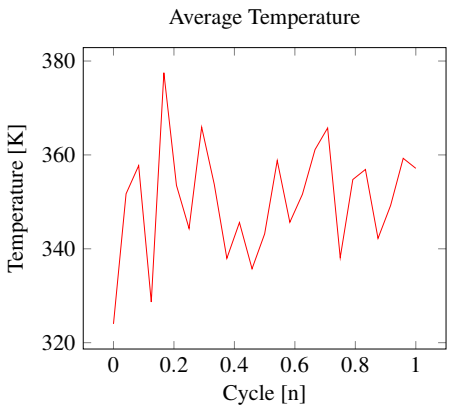

The biggest issue is that the cycle number is unordered, therefore unpredictable and so it is far more important to quickly stop the PCR process. For example, the shortest cycle time was 0.9s (*Note: the number was calculated using previous interaction extrapolation of liquid*). This means that 40 cycles can be done in as little as 6 minutes,

4.2 Convection in an enclosed loop

Even though CCPCR systems are very simple and can work very well, they usually do not produce stable results. They are also hard to control, as even the smallest change in the size of the system can have an enormous impact on stability. Thus, a more sophisticated method was developed. The method includes a closed loop, usually made of pipes. There are many different geometric shapes of such method, including triangles, rectangles, circular, and U shape loops [27]. The sense of control is also given by the fact that the loops are usually heated from 2-4 sides, which establishes a nice uniform convection.

4.2.1 Triangular loop

Triangular CPCR systems are perhaps the most used enclosed loop systems. They are usually designed in a way where three heaters are placed on each side of a triangularly shaped system. The middle is usually empty or a field with an isolating material. Such a system is very stable, but unfortunately quite complex, especially due to a need for a three-heating setup. The design proposed by [28], matches a non-convective PCR performance very well, as the transition between phases almost perfectly matches up the non-convective PCR system. Similar designs were also proposed by [29] and [30]. Let Ω be a triangular domain.

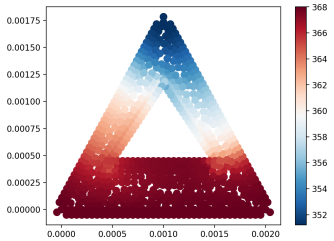

Figure 10. Triangluar CPCR

The convection is very stable. The heat distribution allows the liquid to undergo all three stages equally fast.

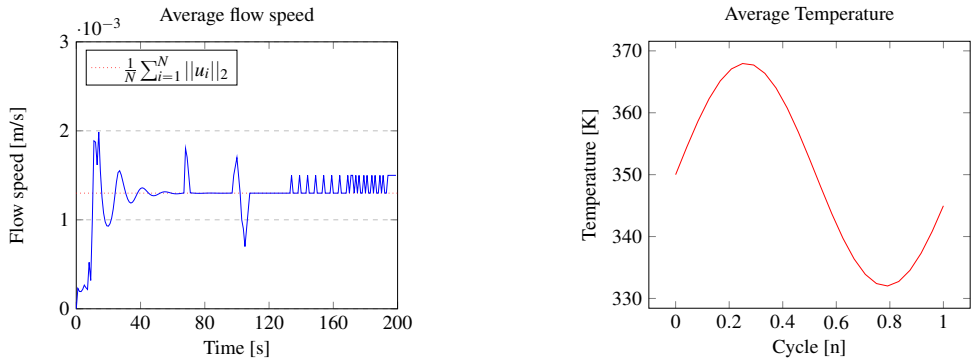

4.2.2 Rectangular and circular loop

The mentioned triangular system is quite complex. Hence, a much less complex system, similar to CCPCR can be used. Both rectangular and circular loop systems have similar performance on small domains, therefore a results from the circular loop will be used. On large domains, circular systems are slightly more stable as suggested by the [31]. We have also compared rectangular and circular domains and found that the circular domain has slightly better stability on domains larger than $D = [0,0.1] \times [0,0.1]$ (*Note: the reason for this might also lie in the numerical method).*

We have slightly adjusted a circular loop design proposed by the study [32]. The systems using rectangular domains have had a fair share of articles, similar designs can be found in almost any paper on CPCR [33] [28]. Let $\Omega = \{(x,y) \in \mathbb{R}^2 : x^2 + y^2 \geqslant 0.007^2 \wedge x,y \leqslant 0.01\}$ be a circular domain and let $\Gamma = \{(x,y) \in \mathbb{R}^2 : 0.007 \leqslant x \leqslant 0.01 \wedge 0.007 \leqslant y \leqslant 0.01\}$ be a rectangular domain. The designs usually use two heaters and so the following boundary conditions are considered

$$\begin{cases} u = \vec{0} \quad \text{on } \partial D \\ T_{top} = 94°C \\ T_{bottom} = 56°C \\ \dfrac{\partial T}{\partial \hat{n}} = 0 \quad \text{on } \partial D_{inner} \wedge \partial D_{left,right} \end{cases} \tag{21}$$

One can also use Robin boundary conditions for the inside boundary.

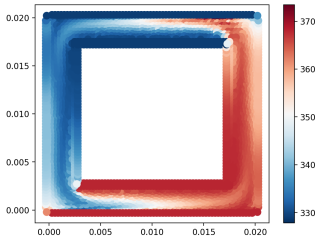

Figure 11. Unstable Rectangular RLCPCR

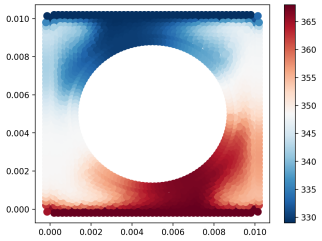

Figure 12. Unstable Circular RL-CPCR

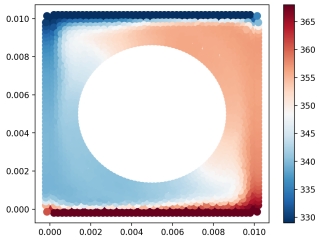

Figure 13. Stable Circular RL-CPCR

Full laminar stability quickly establishes on circular domains as seen by the flow speed graph and Figure 12. Heat distribution only changes slightly after the convection enters a stable phase, thus one can easily predict the speed of a cycle. Our conditions produce short cycles, therefore a slightly larger domain should be considered for better results.

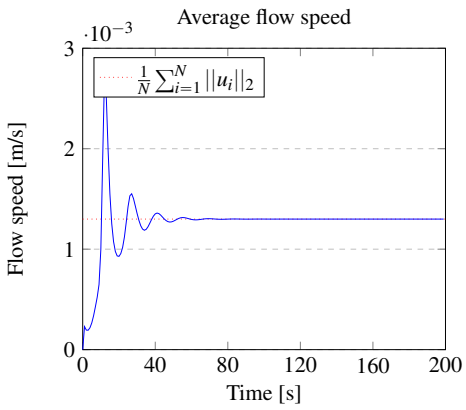

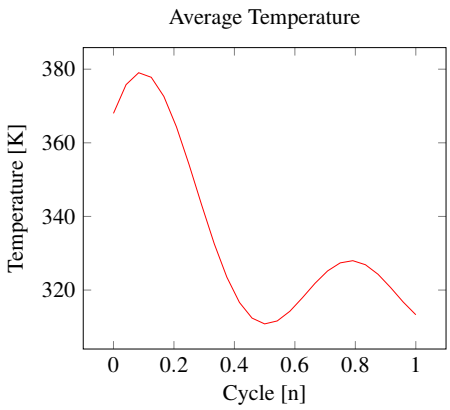

4.3 Convection in a disk

Convection in a disk reactor is used quite rarely. It has only ever been described a couple of times. Namely, in the following articles [34] and [35]. Since the design of the reactor is not widely used, we are not going to analyze it in depth. In short, a heater is placed inside a rectangular or circular system. The design itself is therefore quite complex, but the energy loss might be smaller in comparison to other PCR systems. The convection can also get unstable fairly quickly.

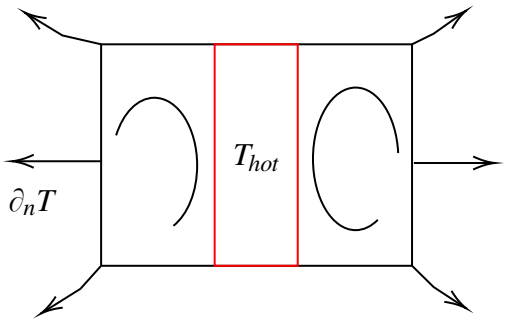

4.4 Performance analysis of the convection systems

Even with gathering a lot of data, it is hard to say which of the designs is the best. The system type choice heavily depends on the specific case. Thus the only logical comparison is heat distribution-based comparison. Moreover, we should compare temperature distribution per cycle between different systems.

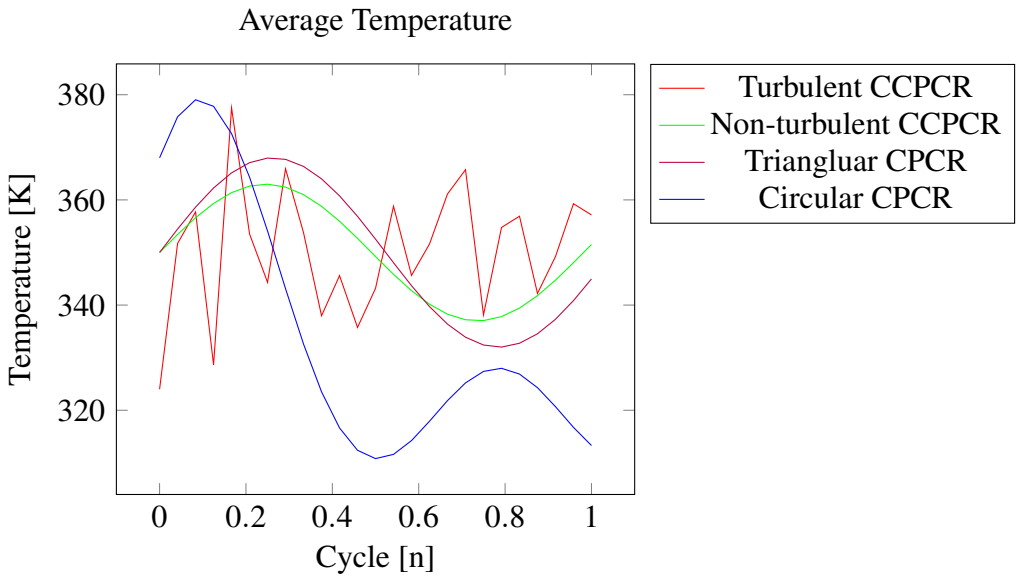

One can see that the output is similar for all laminar designs, thus mainly the stability of the design matters. Furthermore, a loop-based reactor might be used instead of a CCPCR when more liquid and more DNA yield is expected, but even then the CCPCR scheme works well, if and only if it is stable enough.

5. Conclusions

Since the early 2000s, numerous designs for natural convection polymerase chain reaction (PCR) systems have been proposed, leading to continuous improvements over the years. These advancements have brought natural convection PCR reactors to a point where they have surpassed the capabilities of typical (traditional) PCR reactors. In our study, we conducted a thorough analysis of the efficiency of the three most important designs: capillary-tube-based, disk-based, and closed-loop-based CPCR reactors.

The results of our analysis have demonstrated that the simplest C CPCR system produces remarkable efficiency and stability, to the extent that it can replace current non-convective PCRs. Moreover, these CCPCR systems offer cost-efficiency compared to traditional PCR reactors, which can be very expensive. Recent studies have even indicated that capillary tubes, a crucial component in these systems, can be produced at a low cost [36]. Ignoring the price factor, closed-loop CPCR systems can achieve further improvements in efficiency by utilizing closed-loop designs, which are not only highly efficient but also provide ease of control. The high stability of these systems allows for effortless parameter adjustments, including cycle time, velocity, and temperature modifications.

The utilization of computational fluid dynamics(CFD) technology has proven to be highly efficient and accurate in the context of natural convection PCR systems. The difference between simulation results and laboratory conditions is minimal, confirming the reliability and efficacy of CFD simulations. As a result, conducting simulations using the derived system of partial differential equations can facilitate additional enhancements in the technology.

5.1 Further development

While the study has successfully demonstrated the effectiveness of natural convection PCR systems, it is important to note that most of the fluid parameters were disregarded in the analysis. Therefore, future studies can focus on conducting an in-depth analysis of PCR mixture properties and their impact on system performance. Including factors such as fluid viscosity, thermal conductivity, and diffusivity can provide valuable insights into optimizing the efficiency and accuracy of CPCR reactors. By including a comprehensive examination of PCR mixture parameters, we can seek further improvements and thus, higher efficiency of CPCR systems.

REFERENCES

[1] Alexander Morley. Digital pcr: a brief history. *Biomolecular Detection and Quantification*, 96, 09 2014.

[2] Randall K. Saiki, David H. Gelfand, Susanne Stoffel, Stephen J. Scharf, Russell Higuchi, Glenn T. Horn, Kary B. Mullis, and Henry A. Erlich. Primer-directed enzymatic amplification of dna with a thermostable dna polymerase. *Science*, 239(4839):487–491, 1988.

[3] Hanliang Zhu, Haoqing Zhang, Ying Xu, Soňa Laššáková, Marie Korabečná, and Pavel Neuzil. Pcr past, present and future. *BioTechniques*, 69, 08 2020.

[4] *Deoxynucleotide Triphosphates and Buffer Components*, pages 91–101. Springer Netherlands, Dordrecht, 2008.

[5] Xiaofang Wang, Hyun Jeong Lim, and Ahjeong Son. Characterization of denaturation and renaturation of DNA for DNA hybridization. *Environ Health Toxicol*, 29:e2014007, September 2014.

[6] S.E. Atawodi, J.C. Atawodi, and Asabe Dzikwi. Polymerase chain reaction: Theory, practice and application: A review. *Sahel Medical Journal*, 13, 03 2011.

[7] Hyun Jin Hwang, Jeong Hee Kim, and Kyunghoon Jeong. Method and apparatus for amplification of nucleic acid sequences by using thermal convection, December 8 2009. US Patent 7,628,961.

[8] Madhavi Krishnan, Victor Ugaz, and Mark Burns. Pcr in a rayleigh-bénard convection cell. *Science (New York, N.Y.)*, 298:793, 11 2002.

[9] Nam Dinh, Y. Yang, Jiangping Tu, R. Nourgaliev, and Theo Theofanous. Rayleigh-benard natural convection heat transfer: Pattern formation, complexity and predictability. *Proceedings of the 2004 International Congress on Advances in Nuclear Power Plants, ICAPP'04*, 01 2004.

[10] Yash Yadati, Sean McGrath, Atanu Chatterjee, Georgi Georgiev, and Germano Iannacchione. A Detailed Thermodynamic Study of Rayleigh-Benard Cells. In *APS March Meeting Abstracts*, volume 2018 of *APS Meeting Abstracts*, page K47.001, January 2018.

[11] Wen Pin Chou, Ping Hei Chen, Jr Ming Miao, Long Sheng Kuo, Shiou Hwei Yeh, and Pei Jer Chen. Rapid dna amplification in a capillary tube by natural convection with a single isothermal heater. *BioTechniques*, 50(1):52–57, 2011. PMID: 21231923.

[12] Jaka Jakopin Vaupotič Žiga. Analysis of the rayleigh benard convection. 2023.

[13] Dieter Braun, Noel L Goddard, and Albert Libchaber. Exponential dna replication by laminar convection. *Physical review letters*, 91(15):158103, 2003.

[14] Aashish Priye, Yassin A. Hassan, and Victor M. Ugaz. Microscale chaotic advection enables robust convective dna replication. *Analytical Chemistry*, 85(21):10536–10541, Nov 2013.

[15] Radha Muddu, Y. Hassan, and Victor Ugaz. Chaotically accelerated biochemistry in microscale convective flows. *14th International Conference on Miniaturized Systems for Chemistry and Life Sciences 2010, MicroTAS 2010*, 3, 01 2010.

[16] Miha Rot. *Modalna dekompozicija naravne konvekcije v nenewtonskih tekočinah: magistrsko delo*. PhD thesis, [M. Rot], 2020. Bibliografija: str. 47-50.

[17] Benjamin James Hepworth. Nonlinear two-dimensional rayleigh-bénard convection. University of Leeds, March 2014.

[18] Harieth Mhina, Samira Souley Hassane, and Matthew McCurdy. A numerical investigation of rayleigh-benard convection with an obstruction, 2022.

[19] J.H. Ferziger, M. Perić, and R.L. Street. *Computational Methods for Fluid Dynamics*. Springer, 2020.

[20] Upender Kaul. A high-order dissipative scheme for the hyperviscosity-based shock-capturing algorithm. 06 2011.

[21] Jure Slak and Gregor Kosec. Medusa: A c++ library for solving pdes using strong form mesh-free methods. *ACM Transactions on Mathematical Software*, 47:1–25, 06 2021.

[22] Mitja Jančič, Jure Slak, and Gregor Kosec. Monomial augmentation guidelines for rbf-fd from accuracy versus computational time perspective. *Journal of Scientific Computing*, 87(1):9, Feb 2021.

[23] Xianbo Qiu, Jung Il Shu, Oktay Baysal, Jie Wu, Shizhi Qian, Shenxiang Ge, Ke Li, Xiangzhong Ye, Ningshao Xia, and Duli Yu. Real-time capillary convective pcr based on horizontal thermal convection. *Microfluidics and Nanofluidics*, 23:39, 02 2019.

[24] Xianbo Qiu, Shengxiang Ge, Pengfei Gao, Ke Li, Yongliang Yang, Shiyin Zhang, Xiangzhong Ye, Ningshao Xia, and Shizhi Qian. A low-cost and fast real-time pcr system based on capillary convection. *SLAS Technology*, 22(1):13–17, 2017.

[25] V. Kongkaitpaiboon, K. Nanan, and S. Eiamsa-ard. Experimental investigation of heat transfer and turbulent flow friction in a tube fitted with perforated conical-rings. *International Communications in Heat and Mass Transfer*, 37(5):560–567, 2010.

[26] W. Rychlik, W.J. Spencer, and R.E. Rhoads. Optimization of the annealing temperature for DNA amplification in vitro ; . *Nucleic Acids Research*, 18(21):6409–6412, 11 1990.

[27] Guijun Miao, Lulu Zhang, Jing Zhang, Shengxiang Ge, Ningshao Xia, Shizhi Qian, Duli Yu, and Xianbo Qiu. Free convective PCR: From principle study to commercial applications—a critical review. *Analytica Chimica Acta*, 1108:177–197, April 2020.

[28] Zongyuan Chen, Shizhi Qian, William R. Abrams, Daniel Malamud, and Haim H. Bau. Thermosiphon-based pcr reactor: Experiment and modeling. *Analytical Chemistry*, 76(13):3707–3715, 2004. PMID: 15228345.

[29] Nitin Agrawal and Victor Ugaz. A buoyancy-driven compact thermocycler for rapid pcr. *Clinics in laboratory medicine*, 27:215–23, 04 2007.

[30] Nitin Agrawal, Yassin A. Hassan, and Victor M. Ugaz. A pocket-sized convective PCR thermocycler. *Angewandte Chemie International Edition*, 46(23):4316–4319, June 2007.

[31] Chunsun Zhang and Da Xing. Microfluidic gradient PCR (MG-PCR): a new method for microfluidic DNA amplification. *Biomedical Microdevices*, 12(1):1–12, September 2009.

[32] E. K. Wheeler, W. Benett, P. Stratton, J. Richards, A. Chen, A. Christian, K. D. Ness, J. Ortega, L. G. Li, T. H. Weisgraber, K. Goodson, and F. Milanovich. Convectively driven polymerase chain reaction thermal cycler. *Analytical Chemistry*, 76(14):4011–4016, June 2004.

[33] Kwang Hyo Chung, Se Ho Park, and Yo Han Choi. A palmtop PCR system with a disposable polymer chip operated by the thermosiphon effect. *Lab Chip*, 10(2):202–210, 2010.

[34] DIETER BRAUN. PCR BY THERMAL CONVECTION. *Modern Physics Letters B*, 18(16):775–784, July 2004.

[35] Martin Hennig and Dieter Braun. Convective polymerase chain reaction around micro immersion heater. *Applied Physics Letters*, 87(18), October 2005.

[36] Kazuma Kurihara, Ryohei Hokari, and Naoki Takada. Capillary effect enhancement in a plastic capillary tube by nanostructured surface. *Polymers*, 13(4):628, February 2021.